Coronae of stars with supersolar elemental abundances

Peretz[1] U., Behar[1] E., Drake[2] S.A.

[1]Department of Physics, Technion, Haifa 32000, Israel

[2]USRA/CRESST & NASA/GSFC, Greenbelt, Maryland 20771, USA

August 18, 2015

Overview of the First Ionization Potential effect

Coronae of stars with supersolar elemental abundances

Peretz U., Behar E., Drake S.A.

Outline
Overview
Results
Conclusions
Future

Initial FIP effect discovery.

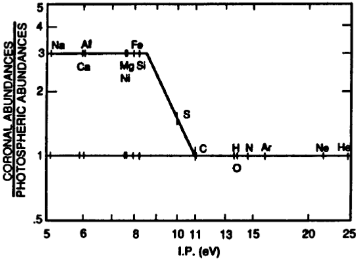

Taken from Feldman (1992). Schematic representation of the solar FIP.

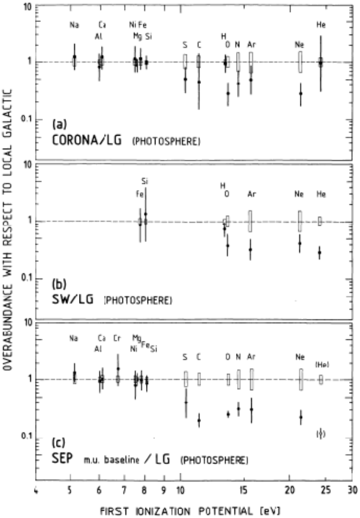

Meyer (1985)

The FIP effect - more history

Newer FIP trends.

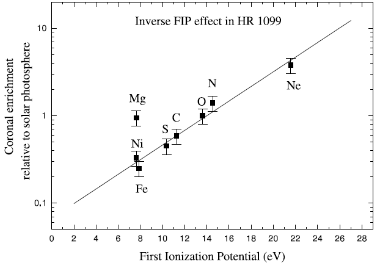

Brinkman et al. (2001)

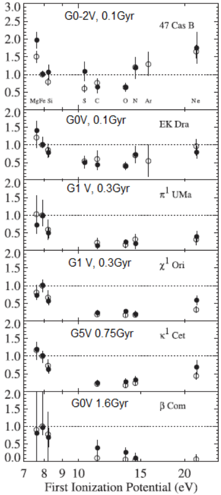

Telleschi et al. (2005)

Motivation

- The physics driving the FIP effect is still unclear
- Much of the FIP analysis is done assuming stellar/solar abundances within examined stars
- Stars with super-solar abundances are the best candidates for observing FIP dependency in varying compositions
- They are also the best candidates for testing the solar assumption

Overview of what we did

- Measure coronal abundances of three **high metallicity** stars previously not measured.
- Collect additional data of previously measured, but not analyzed **high metallicity** stars.
- Determine the FIP trends.
- Compare conclusions based on solar abundances rather than real photospheric measurements.

11LMi spectra

Coronae of stars with supersolar elemental abundances

Peretz U., Behar E., Drake S.A.

Outline

Overview

Results

Spectra

Main results

FIP Bias

Conclusions

Future

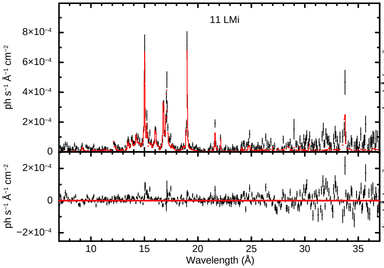

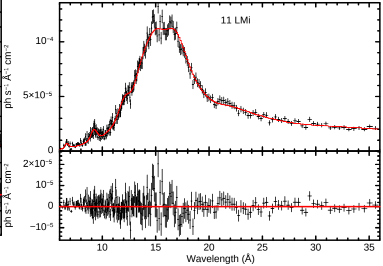

11LMi RGS and EPIC-pn spectra

ι Horologii and HR 7291 spectra

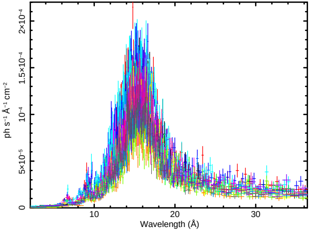

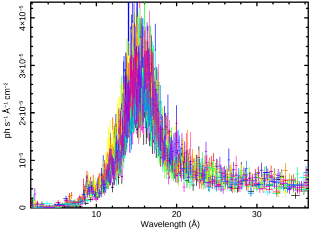

ι Horologii and HR 7291 EPIC-pn spectra

Abundance - Emission Measure degeneracy

Example contour plots fortifying claim absolute abundances may be derived.

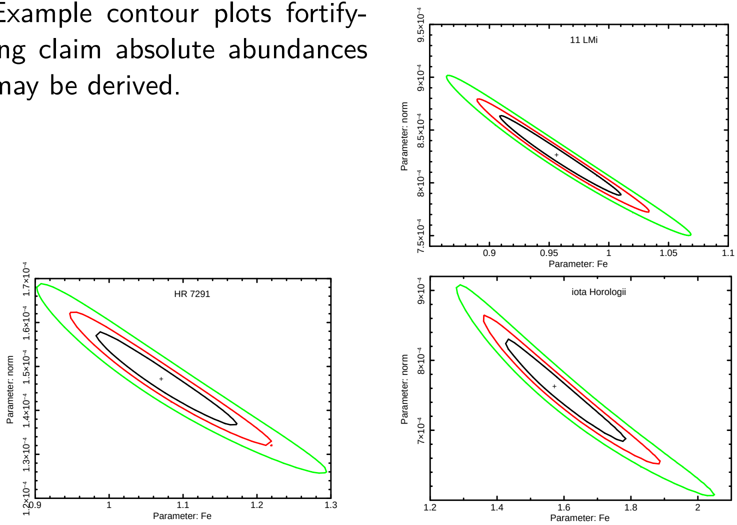

FIP trends

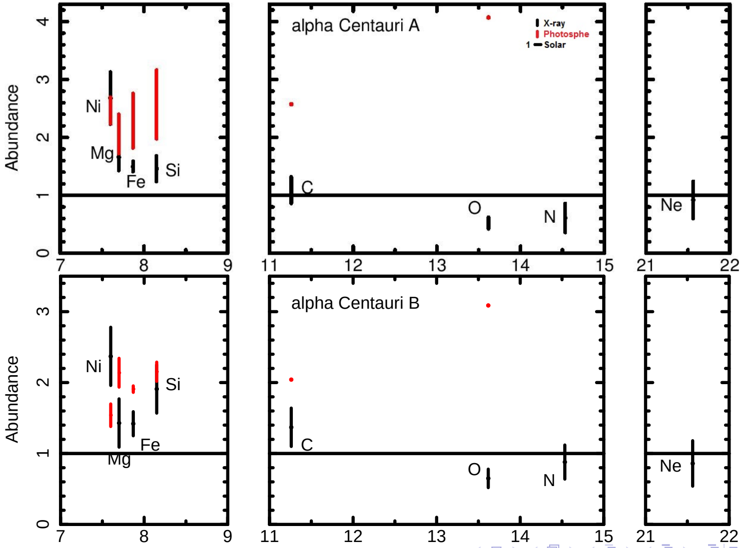
alpha Centauri A
X-ray
Photosphe
1 Solar
Abundance
Ni
Mg
Fe
Si
C
O
N
Ne
alpha Centauri B
0
1
2
3
4
7
8
9
11
12
13
14
15
21
22

The FIP bias

$$FB = \log \frac{(\langle A_{corona}/A_{photo}\rangle)_{low}}{(\langle A_{corona}/A_{photo}\rangle)_{high}}$$

Summary of FIP bias measures

Table: FIP bias measures (uncertainties)

Object	Reference		
	Photospheric	Solar	Wood10[1]
11LMi	0.08(0.38)	0.00(0.43)	0.08(0.44)
ι Horologii	0.38(0.20)	0.31(0.18)	0.54(0.18)
HR 7291	0.50(0.41)	0.32(0.17)	0.92(0.17)
τ Boo	0.42(0.75)	0.23(0.54)	0.28(0.38)
α Centauri A	0.45(0.22)	0.37(0.17)	0.65(0.16)
α Centauri B	0.34(0.20)	0.28(0.16)	0.42(0.18)

[1] Wood & Linsky (2010), $A_{Fe}/ < A_C, A_O, A_N, A_{Ne} >$

The FIP Bias - continued

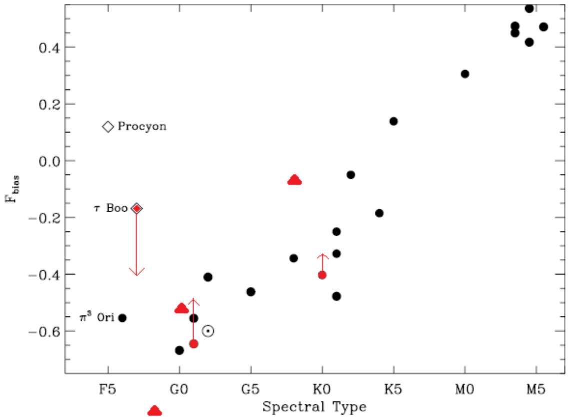

Wood & Linsky (2010); Wood et al. (2012); Wood & Laming (2013)

Conclusions

- We measured the FIP effect in six high metallicity stars
- High depletion regardless of FIP
- Dependence on Spectral type consistent with Wood & Laming (2013)
- True abundances have major implication on FIP research

Looking ahead

- More observations
  - ⋆ Highest metallicity stars
  - ⋆ Larger sample
  - ⋆ Can be done with a CCD spectrometer
  - ⋆ Aim: measuring true FIP trends

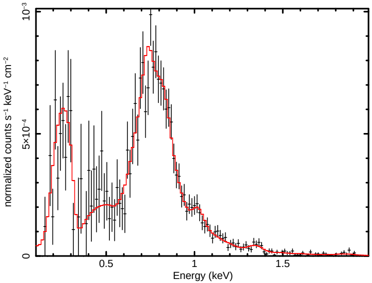

Bibliography

Brinkman, A. C. et al. 2001, A&A, 365, 324

Uri Feldman, 1992, Physica Scripta, 46, 202

Meyer, J. P. 1985, ApJS , 57, 173

Telleschi, A., Güdel, M., Briggs, K., Audard, M., Ness, J.-U., & Skinner, S. L. 2005, ApJ, 622, 653

Wood, B. E. & Linsky, J. L. 2010, ApJ , 717, 1279

Wood, B. E., Laming, J. L., & Karovska, M. 2012, ApJ, 753, 76

Wood, B.E. & Laming, J.M. 2013, ApJ, 768, 122

11 LMi abundances

Table: 11 LMi Summary of Fitted Parameters

Parameter	EPIC-pn Value	Uncertainty 1σ	RGS Value	Uncertainty 1σ
χ^2	273		5375	
DOF	265		5002	
kT_1 [keV]	0.23	0.22-0.24	0.14	0.11-0.19
kT_2 [keV]	0.57	0.55-0.60	0.38	0.34-0.41
kT_3 [keV]			0.69	0.57-0.83
C [solar]	0.1	0.0-4.2	1.1	0.6-1.9
N [solar]	1.5	1.0-3.8	0.6	0.2-1.2
O [solar]	0.4	0.3-0.8	0.8	0.6-1.0
Ne [solar]	0.9	0.5-2.0	0.8	0.6-1.0
Mg [solar]	0.9	0.7-1.5	...	...
Si [solar]	0.6	0.4-0.9	...	...
Fe [solar]	1.0	0.8-1.5	1.0	fixed
Ni [solar]	4.4	2.0-7.1	0.8	0.0-1.9

ι Horologii and HR 7291 abundances

Table: ι Horologii and HR 7291 Summary of Fitted Parameters

Parameter	ι Horologii Value	ι Horologii Uncertainty 1σ	HR7291 Value	HR7291 Uncertainty 1σ
Avg. χ^2	122		117	
Avg. DOF	116		118	
kT_1[keV]	0.26	0.23-0.30		
kT_2[keV]	0.75	0.68-0.81		
O [solar]	0.4	0.3-0.5	0.25	0.2-0.3
Ne [solar]	1.1	0.9-1.3	0.4	0.3-0.5
Mg [solar]	1.9	1.7-2.2	0.9	0.8-1.0
Si [solar]	1.5	1.2-1.7	0.3	0.2-0.4
Fe [solar]	1.3	1.2-1.4	0.8	0.7-0.9

Wood & Laming (2013) trend

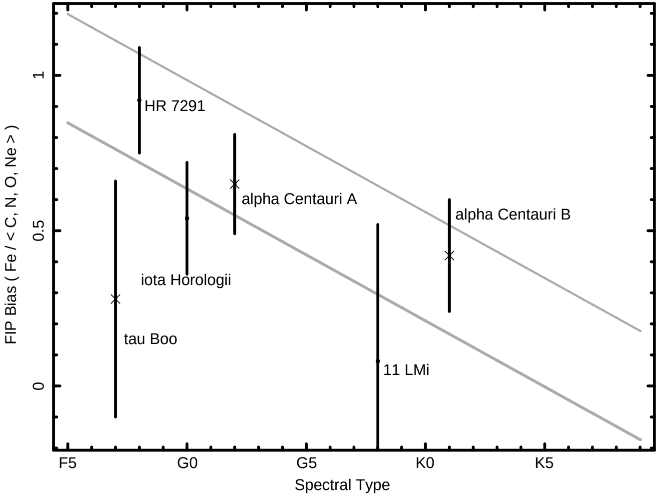

Results using the Wood & Laming (2013) FB. Grey lines represent the observed trend therein.

FIP trends

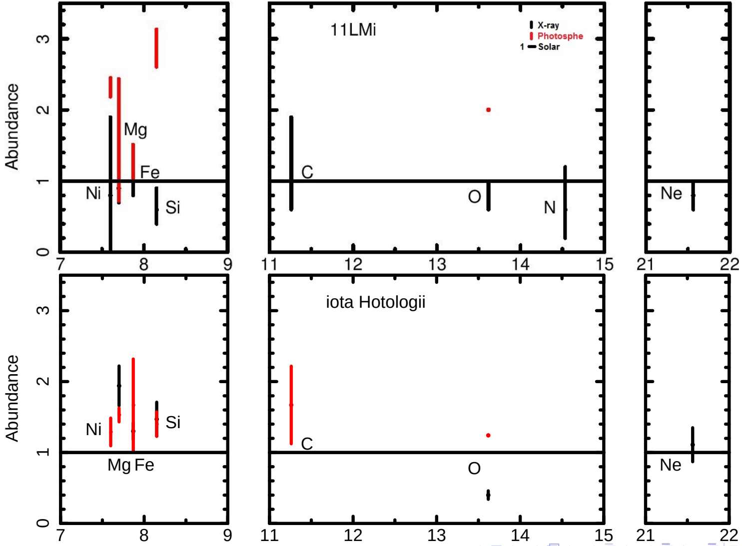
11LMi
X-ray
Photosphe
1 Solar
iota Hotologii
Abundance
Ni
Mg
Fe
Si
C
O
N
Ne
Mg Fe
0
1
2
3
7
8
9
11
12
13
14
15
21
22

FIP trends - continued

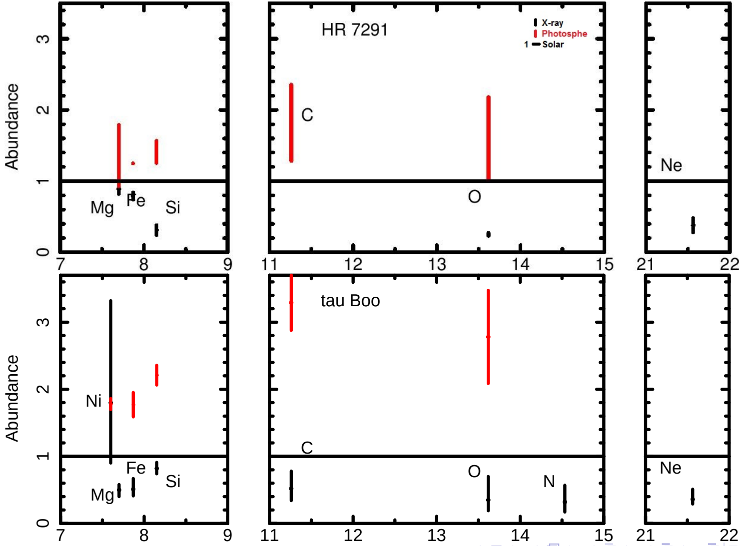

Detailed balance equations in detail

In general for a given **ion**, consider the population density in upper line j, with only electronic processes dominant:

$$\frac{\mathrm{d}n_j}{\mathrm{d}t} = n_e \left(\alpha^l_{l+1} n^{l+1} + S'^l_{l-1} n^{l-1} + \sum_{i>j} Q'^l_{ij} n^l_i + \sum_{i<j} Q^l_{ij} n^l_i - \ldots \right) +$$

$$+ \sum_{k>j} A_{jk} n_k - \sum_{i<j} A_{ij} n_j + \cdots$$

If we consider equilibrium, and invoke additional coronal assumptions:

$$0 = Q_{gj} n_e n_g - \sum_{i<j} A_{ij} n_j \Rightarrow n_j = \frac{Q_{gj} n_e n_g}{\sum_{i<j} A_{ij}}$$

Theoretical spectrum

Define the power spectrum as the total photon density emitted per element ion per energy transition,

$$P_{ij} = A_{ij} n_j = n_e n_g Q_{gj} \frac{A_{ij}}{\sum_{k<j} A_{kj}} =$$

$$= n_e n_H \frac{n_Z}{n_H} \frac{n_{ion}}{n_Z} \frac{n_g}{n_{ion}} Q_{gj} \frac{A_{ij}}{\sum_{k<j} A_{kj}}$$

Define the branching ratio, the abundance A_Z, and G(T), to obtain:

$$P_{ij} = n_e n_H A_Z G(T) BR_{ij}$$

Integrating over the volume of the source we finally get $\frac{\mathrm{ph}}{s}$.